DEVELOPMENT OF A CYCLE-FREE BASED, COORDINATED DYNAMIC SIGNAL-TIMING MODEL FOR MINIMIZING DELAYS

Young-Ihn LEE
Associate Professor, University of Seoul
90 Jeonnong-Dong, Dongdaemun-Gu,
Seoul 130-743, South Korea
Tel. 82-2-2210-2770 Fax. 82-2-2215-5097
E-mail: yilee@uoscc.uos.ac.kr

Wanseok CHOI
Professor, Kwangju University
#592-1, Jinweol-Dong, Nam-Gu,
Kwangju 503-703, South Korea
Tel.82-62-670-2417 Fax. 82-62-670-2190
E-mail: wnskchoi@hosim.kwangju.ac.kr

Jaeseung LIM
Researcher, Urban Science Institute,
University of Seoul
90 Jeonnong-Dong, Dongdaemun-Gu,
Seoul 130-743, South Korea
Tel. 82-2-2210-2302 Fax. 82-2-2215-5097

Abstract: This paper documents the development of a cycle-free signal-timing model for minimizing delays using Genetic Algorithm. The model was embodied using MATLAB, the language of technical computing. A special feature of this model is its ability to manage delays of turning movements on the cycle basis. The model produces a cycle-free based signal timing(cycles and green times) for each intersection to minimize delays of turning movements on the cycle basis. Concurrently, appropriate offsets could be accomplished by applying cycle-free based signal timings for respective intersections. The model was applied to an example network that consists of four intersections. The result shows that the model produces superior signal timings to the existing signal timing model in terms of managing delays of turning movements.

Key Words: Cycle-free, Signal Control, Minimizing Delay, and Genetic Algorithm

1. INTRODUCTION

The area of developing efficient and effective real-time traffic control systems might be one of the leading areas of the traffic control fields. State-of-the-art concepts of traffic-responsive control in urban streets network consist of the three generations of the Urban Traffic Control System (UTCS).

First-generation control uses prestored signal timing plans developed off-line and based on historical traffic data. The signal timing plan can be mainly selected on the basis of time-of-day, or by matching a signal timing pattern that is fitted to recently measured traffic conditions. A network threshold value that incorporates traffic volumes and occupancies can be used for the matching criterion. In the traffic-responsive mode, the allocation of green time (split) can be slightly adjusted based on fluctuations in local traffic demand.

As an alternative to the off-line signal timing plans, Second-generation control was developed as an online model that computes and implements signal timing plans in a cycle-by-cycle basis. The signal timings could be changed at 5- to 10-min intervals based on surveillance data gathered from vehicle detectors and predicted traffic volumes(1). Second-generation control has the capability for dynamically decomposing the network into subnetworks that consist of 1 to 10 intersections on the basis of traffic conditions. Each subnetwork contains one critical intersection, and optimal signal timings for the subnetwork are computed based on the traffic conditions of the critical intersection.

The Third-generation control strategy is developed to control traffic flows in a real time basis(2-6). The overall objective of Third-generation control is to provide the utmost in control responsiveness and flexibility. To accomplish this goal, Third-generation control was designed to allow the signal control variables such as cycle length, green time, and offset to change continuously in response to real-time measurements of traffic variables. It means that cycle length, green time, and offset of an intersection are permitted to vary both specially and temporally to provide progressive movement of traffic and to minimize system disutility. Third-generation control strategy was implemented at Washington DC. in 1974, however, numerous problems associated with maintenance and transition-related deficiencies forced to not continue the research.

The purpose of this study is to setup a signal optimization procedure using genetic algorithm and to develop a cycle free signal-timing model based on Third-generation control concept.

2. NOTATION

The notation of variables in this paper are defined as follows:

k : the number of turning movement, NEMA type($1 <= k <= 8$)
i : the number of intersection($1 <= i <= 4$)
n : the number of cycle (integer)
$g_i^k(n)$: green time of movement k (sec, intersection i, n-th cycle)
$s_i^k(n)$: the time of saturated departure flow pattern (movement k, intersection i, n-th cycle)
$C_i(n)$: cycle length (sec, intersection i, n-th cycle)
$T_S^k(n)$: saturated departure rate of upstream movement #2 (input of movement k at intersection i):
$T_A^k(n)$: average departure rate of upstream movement #2 (input of movement k at intersection i)
$L_S^k(n)$: saturated departure rate of upstream movement #7 (input of movement k at intersection i)
$L_A^k(n)$: average departure rate of upstream movement #2 (input of movement k at intersection i)
$R_A^k(n)$: average departure rate of upstream right turn movements (input of movement k at intersection i)
Q_{int}^k : initial queue length of movement k at the beginning of cycle
Q_s^k : queue length of movement k at the start of green time.
Q_E^k : queue length of movement k at the end of green time.
TD_E^k : traffic demand for movement k at the end of green time.
TD_s^k : traffic demand for movement k at the start of green time.
X_i^k : degree of saturation (movement k, intersection i) $X_i^k = (v_i/c_i) = (v_i/s_i) \times g_i^k/C_i(n))$
V^k : turning volume (movement k, intersection i)
D^k : average delay (movement k, intersection i)

Test network consists of four intersections: two external intersections and two internal intersections. Arrival rates of external movements are assumed to be constant (uniform arrival) and platoon dispersion is not considered in this research. Phase sequence is assumed to be Lead-Lead pattern. The configurations of the test network and phase sequence are shown as figures 1 and 2.

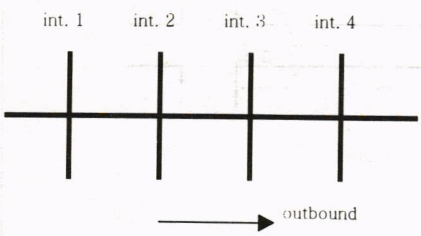

<Figure 1> Configuration of Test network

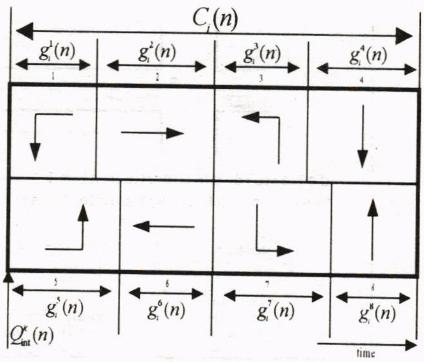

<Figure 2> Phase Sequence (Lead-Lead pattern)

3. ALGORITHM DESCRIPTION

3.1 Traffic Flows

The proposed model simulates traffic flow macroscopically. The green time is divided into two time increments of variable duration: (1) the time for saturation departure pattern (queue dissipation time) and (2) the time for average flow pattern. Each time of flow pattern is identified by its start and end times. There are two traffic flow patterns: the IN and OUT patterns.

The IN pattern is the arrival pattern, including the arrivals at the stop line if traffic is not impeded by the downstream signal. It is assumed that the IN pattern for external (network input) links or mid-block input flows is always a uniform distribution. For internal links, the IN pattern is assumed not to be affected by the platoon dispersion.

The OUT pattern is the flow pattern that would leave the stop line if there are enough traffic to saturate the green (see figure 3). After the queue dissipates, it is equal to the IN pattern for the duration of the effective green. To determine the OUT pattern, the queue at the start of the green time must first be determined.

Figure 3 demonstrates flow patterns of this research. The arrival patterns of an intersection are equal to the departure patterns of the upstream intersection. The time of saturation departure patterns of the intersection, queue dissipation time, is calculated by adding the number of vehicles arrived at the intersection during the time of saturation departure patterns to the number of queued vehicles at the start of the green time. The shadowed area of the IN pattern is equal to the shadowed area of the OUT pattern in Figure 3.

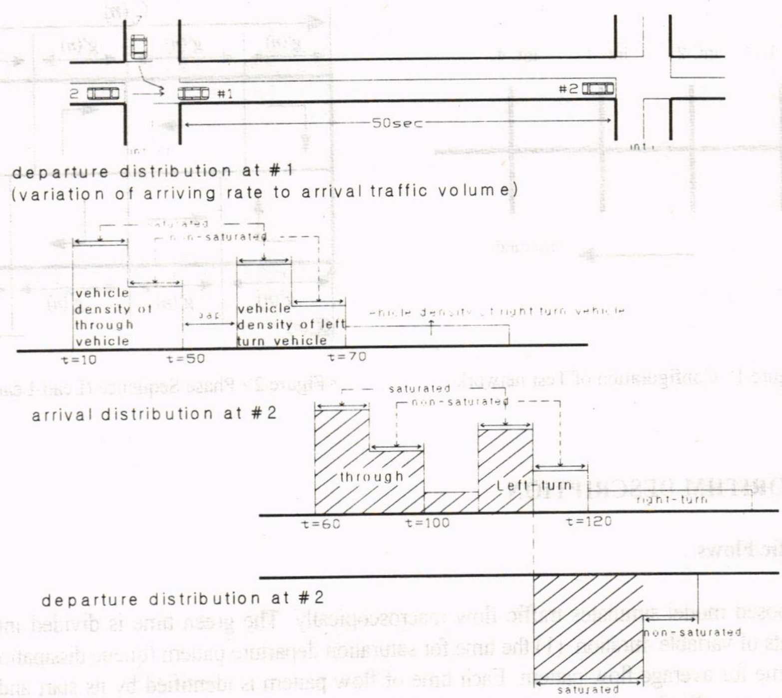

<Figure 3> Concept of Arrival and Departure Flow Patterns

3.2 Objective Functions for Minimizing Delays

The primary measurement of effectiveness of the model is average delay. The HCM delay function was applied in this research. Delay is composed of a uniform element, a random element, and the delay due to oversaturation. The uniform delay is calculated by averaging the queue length over the cycle. Random and saturation delay is not considered in the model. In the dynamic signal timing process, the delay experienced by the vehicle arriving at the intersection during the red time should be considered. Thus, total delay is computed as follows:

$$d = d_1 \times DF + D_E \quad \text{------------------------------} (1)$$

where, $d_1 = 0.38 \times C \times \frac{(1-g_i/C)^2}{[1-(g_i/C)\times X_i]}$, uniform delay

$DF = 1.0$

D_E = the delay experienced by the vehicle arriving at the intersection during the red time

$$D_E = [(Q_E^-(n-1) \times [g_i^{'}(n-1) + g^{-}(n-1) + g_i^{'}(n)]) + (\lambda_R + \lambda_T + \lambda_L) \times [g_i^{'}(n-1) + g_i^{+}(n-1) + g_i^{'}(n)]^2 \div 2)] / V$$

$$d_i = \frac{\sum d_i V_i}{\sum V_i} \qquad d_A = \frac{\sum d_A V_A}{\sum V_A}$$

V : traffic volume for movement i .

d_i : average delay for intersection i .

Usually the major traffic flows determine the purpose of the signal system. On a two-way arterial network such as the test network, the movements to be progressed should be considered in the signal system. In the research, three objective functions were setup considering the movements to be progressed; inbound, outbound, and both movements to be progressed. The objective functions are as follows:

(1) Objective function for balanced movements

$$FV_B^d = \frac{(D^1 \cdot V^1 + D^2 \cdot V^2 + D^5 \cdot V^5 + D^6 \cdot V^6)}{(V^1 + V^2 + V^5 + V^6)} \quad \text{-------------------------------- (2)}$$

(2) Objective function for inbound movements

$$FV_I^d = \frac{D^6 V^6}{V^6} \quad \text{-------------------------------- (3)}$$

(3) Objective function for outbound movements

$$FV_O^d = \frac{D^2 V^2}{V^2} \quad \text{-------------------------------- (4)}$$

where, FV : objective function

D^k : average delay for movement k

V^k : traffic volume for movement k

3.3 Mathematical Representation of the Algorithm

The mathematical representation of the cycle-free optimization algorithm is as follows:

Find C, G_{ij}

$$Min \;\; Z_d(P) \quad \text{-------------------------------- (5)}$$

$$Min \;\; FV^d = \frac{\sum_{k=1}^{8} D_i^k}{\sum_{k=1}^{8} V_i^k} \quad \text{-------------------------------- (6)}$$

$$FV_B^d = \frac{(D^1 \cdot V^1 + D^2 \cdot V^2 + D^5 \cdot V^5 + D^6 \cdot V^6)}{(V^1 + V^2 + V^5 + V^6)} \quad \text{-------------------------------- (7)}$$

$$FV_I^d = \frac{D^6 V^6}{V^6} \quad \text{-------------------------------- (8)}$$

$$FV_O^d = \frac{D^2 V^2}{V^2} \quad \text{-------------------------------- (9)}$$

subject to

$G_{i1} + G_{i2} = G_{i5} + G_{i6}$, for i = 1, ..., N

$G_{i3} + G_{i4} = G_{i7} + G_{i8}$, for i = 1, ..., N

$\sum G_{ij} = C$ for i = 1, ..., N

$G_{ij} \geq MG_{ij}$ for i = 1, ..., N and for j = 1, ..., N

$Min \; C \leq C \leq Max \; C$, G, $C \geq 0$ and $integer$

3.4 Delay Calculation for External Movements

In this section, the calculation process of average delay for external movements is demonstrated. For instance, average delay for external movements (movement #2, intersection #1) is estimated based on the number of queued vehicles at the beginning of the cycle, Q_{int}^2 (n) , and the arrival flow rate, lambda . Traffic demand for external movement # 2 is estimated by adding arrival demand in current cycle to the queued vehicles at the beginning of the cycle. Thus, average delay for external movement # 2 is calculated as follows:

$$TD_E^2 = Q_{int}^2(n) + \lambda\{g_i^1(n) + g_i^2(n)\}$$
$$= Q_E^2(n-1) + \lambda\{g_i^3(n-1) + g_i^4(n-1)\} + \lambda\{g_i^1(n) + g_i^2(n)\} \quad \text{------------------------- (10)}$$

$$C_i(n) = g_i^1(n) + g_i^2(n) + g_i^3(n) + g_i^4(n) \quad \text{------------------------- (11)}$$

$$X_i^2 = V^2/(S_i \times (g_i^2/C_i(n))) \quad \text{------------------------- (12)}$$

$$D_i^2 = \left(0.38 \times C_i(n) \times \frac{(1 - g_i^2/C_i(n))^2}{\{1 - (1 - g_i^2/C_i(n))\} \times X_i^2}\right) + [(Q_E^2(n-1) \times [g_i^3(n-1) + g_i^4(n-1) + g_i^1(n)]$$
$$+ (\lambda_E + \lambda_w + \lambda_L) \times [g_i^3(n-1) + g_i^4(n-1) + g_i^1(n)]^2 \div 2] / V^2 \quad \text{------------------------- (13)}$$

where, $\left(X_i^2 = \frac{[Q_E^2(n-1) + \lambda\{g_i^3(n-1) + g_i^4(n-1)\}}{(S \times g_i^2/C_i(n))} + \frac{\lambda\{g_i^1(n) + g_i^2(n)\} \times (3600/C_i(n))}{(S \times g_i^2/C_i(n))}\right)$

3.5 Delay Calculation for Mid-block Movements

Average delay for mid-block movements (movement #2, intersection #1) should be expressed by the function of time. The arrival time of upstream feeding flows and green time of movement #2 are varied depending on the signal timing plans. Figure 4 shows the arrival and departure patterns of mid-block movement #2 at internal intersection. Because of uniform distribution of traffic flows, the arrival pattern of an intersection is equal to the departure pattern of the upstream intersection. The traffic demand for movement # 2 (area in figure 4) can be calculated by the following unit step function.

$$f(t) = R_A^k(n-1) \times u(t - t_1^k) + T_S^k(n-1) \times u(t - t_2^k)$$
$$+ \{T_A^k(n-1) - T_S^k(n-1)\} \times u(t - t_3^k) - T_A^k(n-1) \times u(t - t_4^k) + L_S^k(n-1) \times u(t - t_5^k) + \{L_A^k(n-1) - L_S^k(n-1)\} \times u(t - t_6^k)$$
$$- L_A^k(n-1) \times u(t - t_7^k) + \{R_A^k(n) - R_A^k(n-1)\} \times u(t - t_8^k) + T_S^k(n) \times u(t - t_9^k) + \{T_A^k(n-1) - T_S^k(n)\} \times u(t - t_{10}^k) - T_A^k(n)$$
$$\times u(t - t_{11}^k) + L_S^k(n) \times u(t - t_{12}^k) + \{L_A^k(n) - L_S^k(n)\} \times u(t - t_{13}^k) - L_A^k(n) \times u(t - t_{14}^k) + T_S^k(n) \times u(t - t_{15}^k) + \{T_A^k(n) - T_S^k(n)\}$$
$$\times u(t - t_{17}^k) - T_A^k(n) \times u(t - t_{18}^k) + L_S^k(n) \times u(t - t_{19}^k) + \{L_A^k(n) - L_S^k(n)\} \times u(t - t_{20}^k) - L_A^k(n) \times u(t - t_{21}^k) - R_A^k(n) \times u(t - t_{22}^k) \quad (14)$$

thus, $f(t) = \sum_{j=1}^{22} a_j \times u(t - t_j^k)$ ------------------------- (15)

where, if $t_j^k < 0$, then $t_j^k = 0$ $(j = 1 \text{ to } 22)$

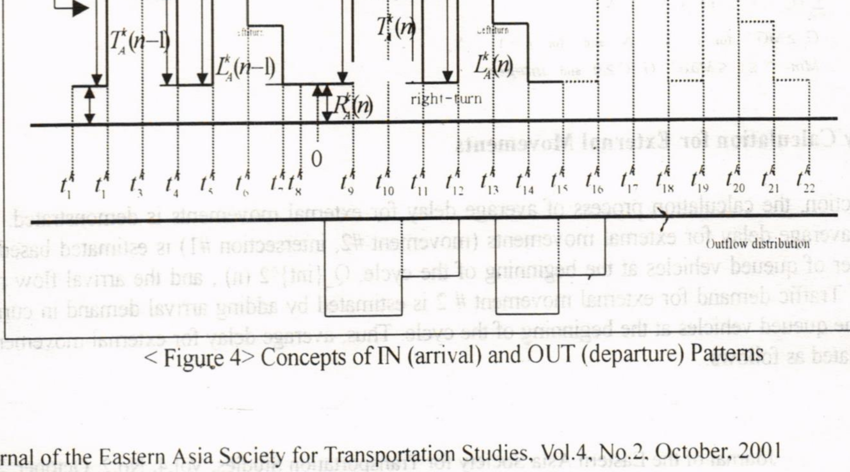

< Figure 4> Concepts of IN (arrival) and OUT (departure) Patterns

When the green time of movement # 2 is from t_s^2 to t_e^2 in figure 4, average delay for the movement #2 can be estimated by following equations.

$$D_i^2 = d_i^2 \times DF^2 = d_i^2 + D_B^2 \quad \text{-------------------------------- (16)}$$

$$D_i^2 = \left(0.38 \times (C_i(n) \times \frac{(1 - g_i^2 / C_i(n))^2}{[1 - (g_i^2 / C_i(n)) \times X_i^2]} \right) + ([Q_B^2(n-1) \times [g_i^1(n-1) + g_i^4(n-1) + g_i^2(n)] + [(\lambda_{TS} \times (t_{TS}^2 - t_e^2)^2 \div 2) \times (t_s^2 - t_{TS}^2)$$

$$+ (\lambda_{TA}(t_{TA}^2 - t_{TS}^2)^2 \div 2) \times (t_s^2 - t_{TA}^2) + (\lambda_{LS}(t_{LS}^2 - t_s^2)^2 \div 2) \times (t_s^2 - t_{LS}^2) + (\lambda_{LA} \times (t_{LA}^2 - t_{LS}^2)^2 \div 2) \times (t_s^2 - t_{LA}^2) + \lambda_{RA}(t_{RA}^2 - t_s^2)^2 \div 2]]) / V_i^2 \quad \text{---- (17)}$$

where, $f_k(t)$ = traffic demand

$Q_{\text{int}}^k = Q_B^k(n-1) + \int_{t_g^k(n-1)}^{C(n-1)} f_k(t)dt$. number of queued vehicles at the beginning of green time

$X_i^2 = \dfrac{V_i^2}{S \times (\frac{g_i^2}{C_i(n)})}$, degree of saturation, $\left[X_i^2 = \dfrac{\left[Q_B^2(n-1) + \int_{t_g^2(n-1)}^{C(n-1)} f_2(t)dt + (\int_0^{t_g^2} f_2(t)dt)\right] \times \left(\frac{3600}{C_i(n)}\right)}{S_i \times (g_i^2 / C_i(n))} \right]$

$$V_i^2 = \left[Q_B^k(n-1) + \int_{t_g^k(n-1)}^{C(n-1)} f_k(t)dt + \left(\int_0^{t_g^k} f_2(t)dt \right) \right] \times \left(\frac{3600}{C_i(n)} \right)$$

3.6 Coding and Decoding Process in Genetic Algorithm

Genetic Algorithms have considerable advantages when applying it to the signal optimization process. In Genetic Algorithm encoding is carried out using binary strings. One of the most complex problem for applying Genetic Algorithms to the constrained optimization is how to handle constraints. Genetic operators used to manipulate the chromosomes often yields infeasible offspring. Several techniques have been applied to handle signal constraints with Genetic Algorithms. In this study, a fraction-based decoding scheme is applied to handle the signal timing constraints. Figure 5 illustrates the fraction-based decoding scheme.

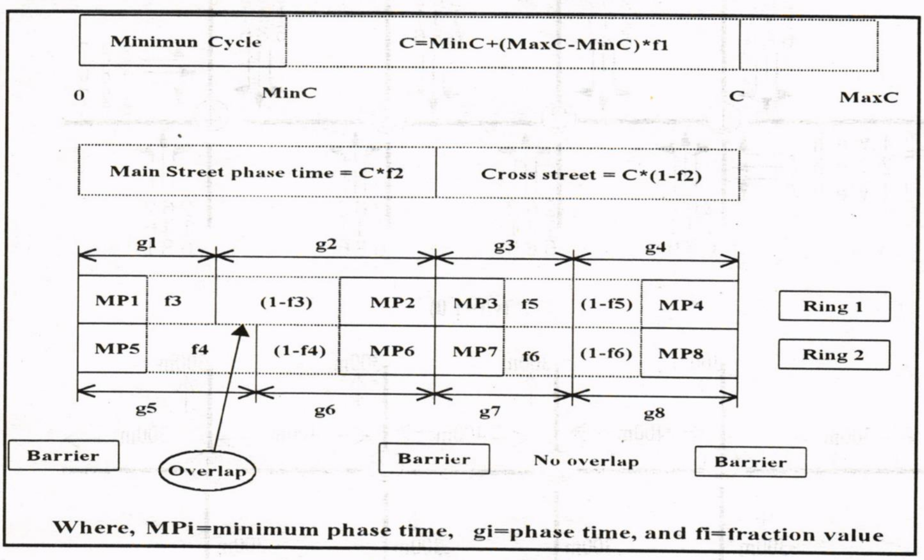

<Figure 5> A fraction-based decoding scheme

(source: Park B. K., "Development of Genetic Algorithm-Based Signal Optimization Program for Oversaturated Intersection", Texas A&M University, 1998.)

4. DESIGN OF EXPERIMENT

4.1 Test network

The proposed model was tested on a arterial network consists of 4 intersections. The traffic conditions are as follows:

- number of lanes: right-turn, through, and left-turn lanes
- phase sequence: Lead-Lead sequences, dual ring NEMA types
- minimum cycle length 70-sec. maximum cycle length 160 sec.
- minimum green - main stream (East↔West) through movements: 25 sec.
  - cross street through movements and left-turning movements: 15 sec
- initial number of queues: 5 vehicles for each external movement
- saturation flow rate: 1,800vph
- link traversing speed: 36km/h (10m/sec)
- Yellow time: 3 sec.
- simulation time: 30 minutes

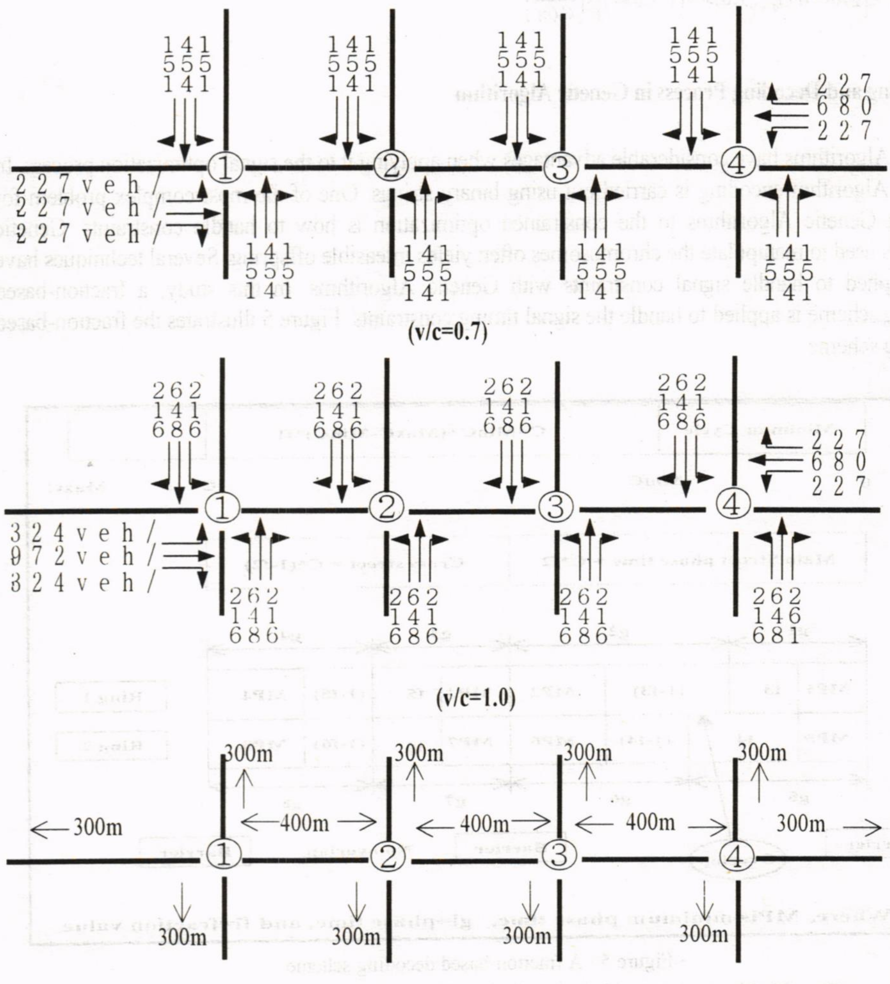

<Figure 6> Turning Volumes and Network Geometrics

4.2 Model Programming

The model was embodied using MATLAB, the language of technical computing. LP produced the Initial signal timings for intersections in MATLAB library. Figure 7 shows the flow of the cycle free signal timing approach within the MATLAB programming.

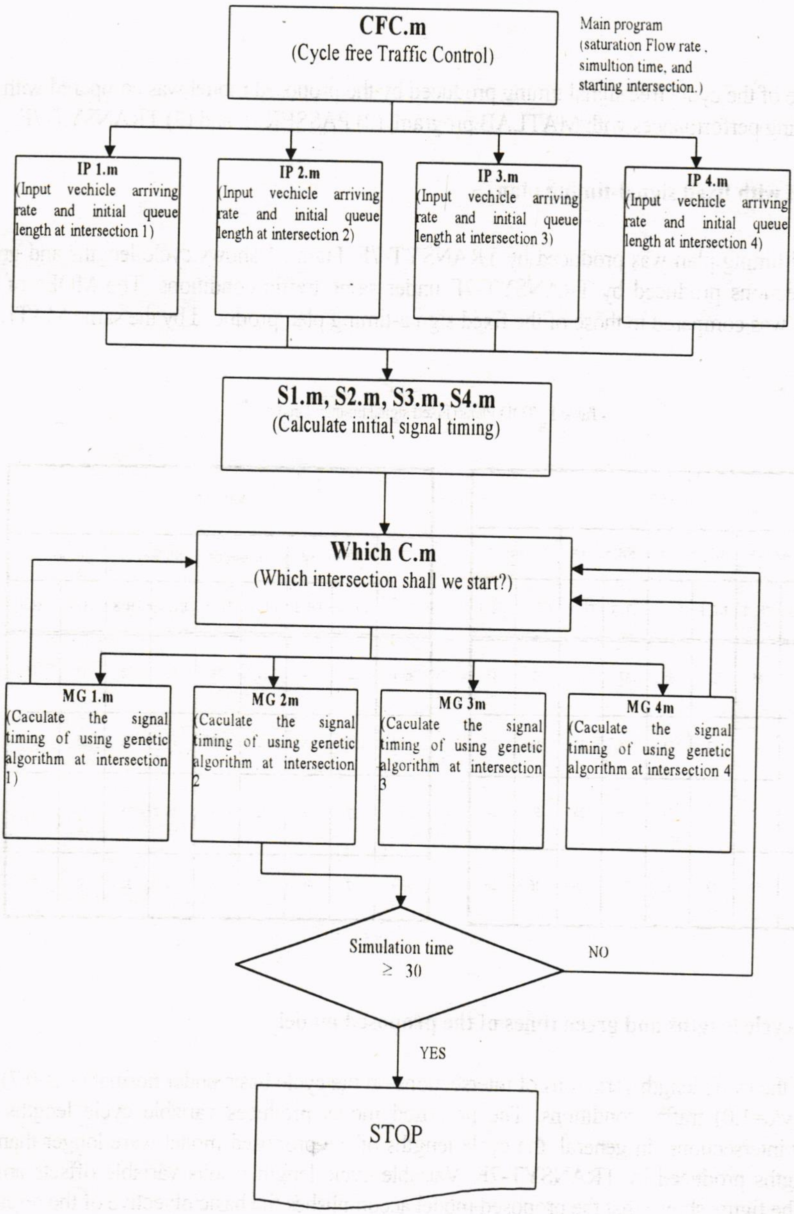

<Figure 7> Flow chart of the Cycle-free signal timing model

4.3 Measures of Effectiveness

The model provides various MOEs to represent traffic conditions in given control strategies. The performance of the cycle-free signal timings was evaluated in movement-by-movement comparisons. The methods for measuring model performance are (1) the number of queued vehicles at the end of green time for each movement, and (2) the number of vehicles passing through the intersection.

5. RESULTS

The performance of the cycle free signal timing produced by the proposed model was compared with (1) Fixed signal timing performances with MATLAB program, (2) PASSER II, and (3) TRANSYT-7F.

5.1 Comparison with fixed signal-timing plan

The fixed signal timing plan was produced by TRANSYT-7F. Figure 1 shows cycle lengths and green times for intersections produced by TRANSYT-7F under same traffic conditions. The MOEs of the proposed model was compared to those of the fixed signal-timing plan produced by the same MATLAB program.

<Table 1> TOD Plans (Fixed signal timing plans)

V/C = 0.7								
Int. #	EB. mov't #		WB. mov't #		NB. mov't #		SB. mov't #	
	LT. 5	TH. 2	LT. 1	TH. 6	LT. 3	TH. 8	LT. 7	TH. 4
Int 1	21	65	21	65	37	37	37	37
Int 2	17	51	17	51	26	26	26	26
Int 3	17	51	17	51	26	26	26	26
Int 4	17	51	17	51	26	26	26	26

V/C = 1.0								
Int. #	EB. mov't #		WB. mov't #		NB. mov't #		SB. mov't #	
	LT. 5	TH. 2	LT. 1	TH. 6	LT. 3	TH. 8	LT. 7	TH. 4
int 1	22	74	22	74	32	32	32	32
int 2	22	68	22	68	35	35	35	35
int 3	22	68	22	68	35	35	35	35
int 4	22	68	22	68	35	35	35	35

5.1.1 Variable cycle lengths and green times of the proposed model

Figure 8 shows the cycle length variations of intersections on the cycle basis under normal (v/c=0.7) and oversaturated (v/c=1.0) traffic conditions. The proposed model produces variable cycle lengths and green times for intersections. In general, the cycle lengths of the proposed model were longer than the fixed cycle lengths produced by TRANSYT-7F. Variable cycle length results variable offsets among intersections. The figure shows that the proposed model accomplishes the basic objective of the research, producing cycle free signal timings on the cycle basis.

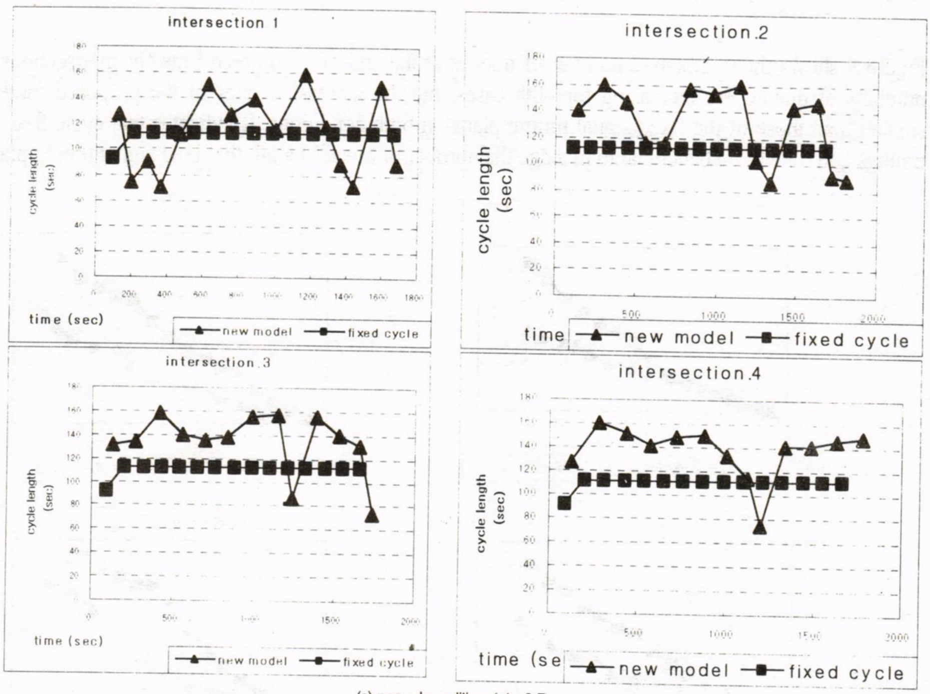

(a) normal conditions(v/c=0.7)

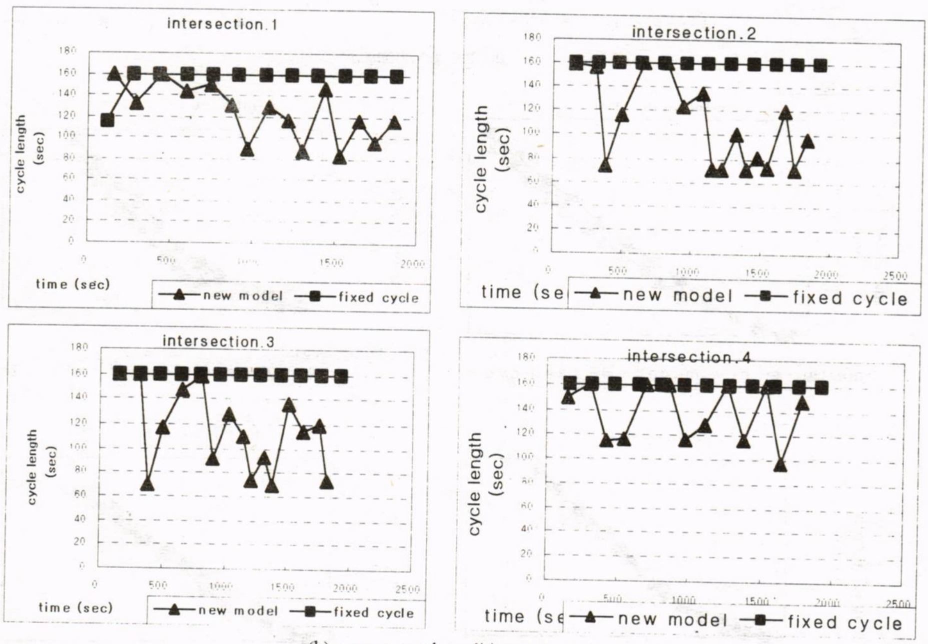

(b) oversaturated conditions (v/c=1.0)

<Figure 8> variation of cycle lengths

5.1.2 Number of queues

Figure 9 shows the cumulative number of queues at the end of each green time for intersections. The numbers of queues are increasing for both cases, but the increasing rates of the proposed model are smaller than those of the fixed signal timing plans on both conditions. It indicates that cycle free signal timings could be more beneficial to manage the number of queues length the fixed signal timing plans.

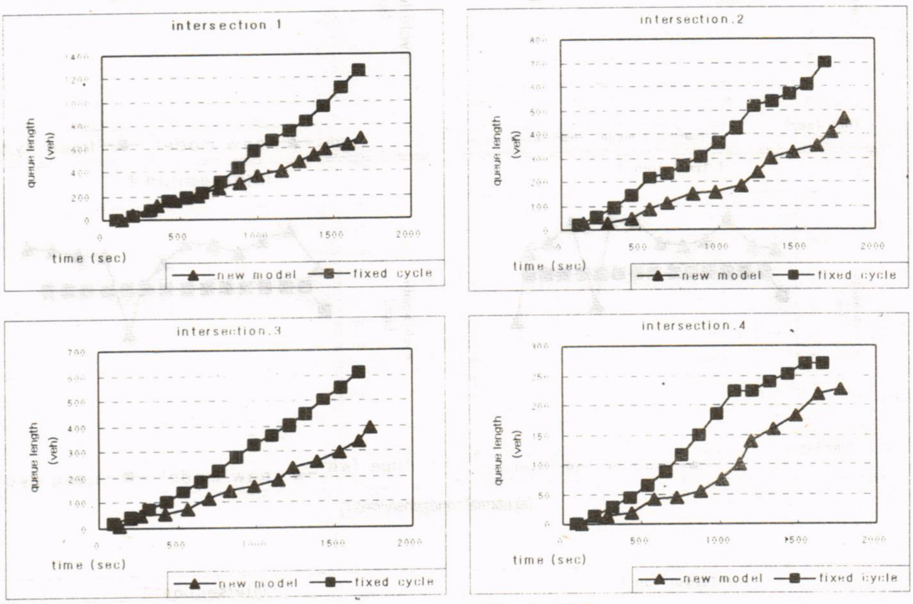

(a) normal conditions(v/c=0.7)

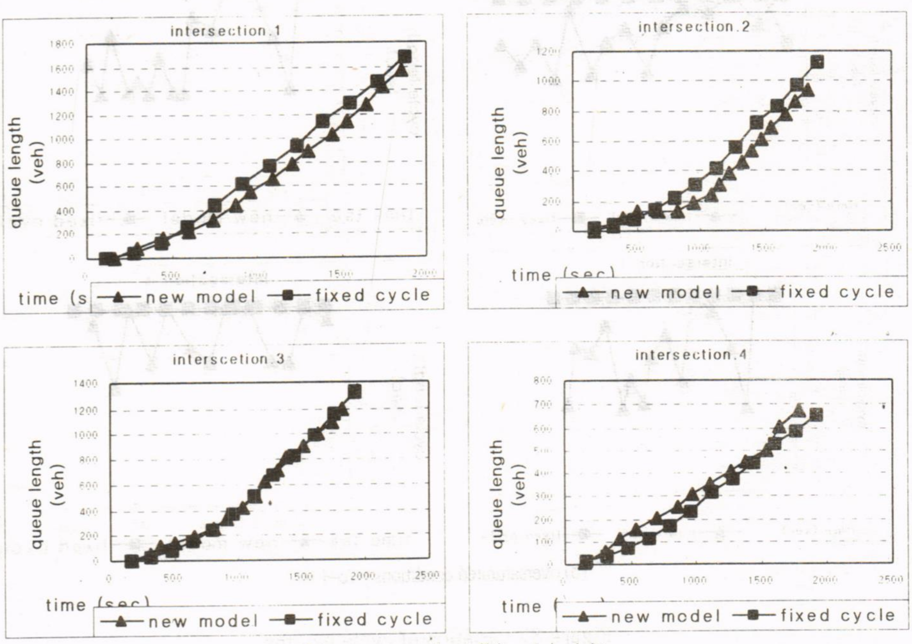

(b) oversaturated conditions(v/c=1.0)

<Figure 9> queue length accumulations

5.1.3 Throughputs

Figure 10 shows the cumulative number of throughput for intersections. On normal condition, the proposed model allows slightly more vehicles passing through the test network, but the cumulative numbers of throughputs are almost same for both cases. It means that most of vehicles can passing through the network under normal conditions. On oversaturated conditions, the proposed model allows more throughput than the fixed signal timing. It shows that the cycle free signal timing is superior to the fixed signal timing to manage oversaturated traffic flows of intersections.

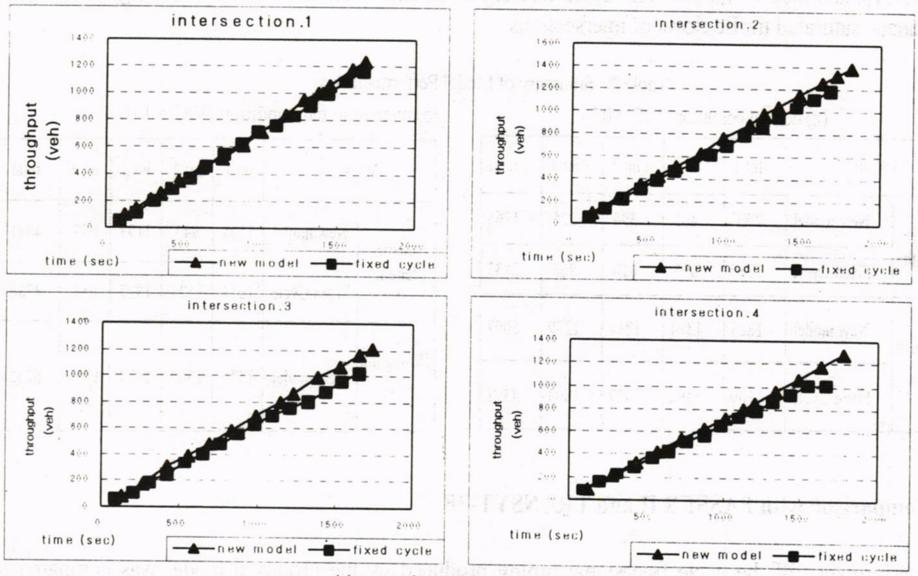

(a) normal conditions(v/c=0.7)

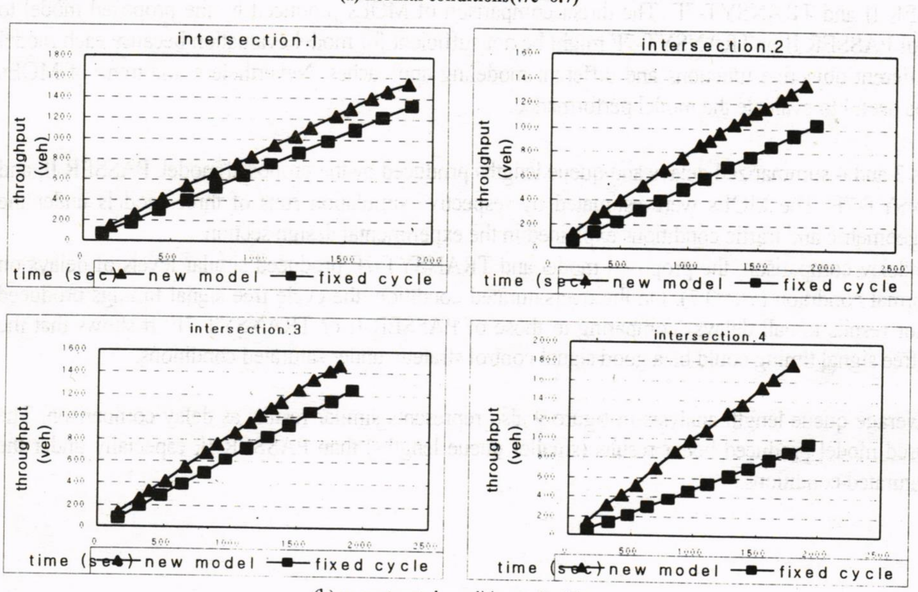

(b) oversaturated conditions(v/c=1.0)

<Figure 10> Throughput Accumulations

5.1.4 Summary

Queue lengths and throughputs produced by the cycle free signal timing and the fixed signal timing are summarized in table 2. The result shows that

(1) the proposed model accomplishes the basic objective of the research, producing cycle free signal timings on the cycle basis.
(2) On Normal conditions, Even though most of vehicles can pass through the network, cycle free signal timings could be more beneficial to manage traffic flows in the viewpoint of managing queue lengths.
(3) On oversaturated conditions, the cycle free signal timing is superior to the fixed signal timing to manage saturated traffic flows of intersections

<Table 2> Summary of Model Performances

(a) normal condition (V/C = 0.7)

V/C=0.7		Int 1	int 2	int 3	int 4	total
queue length	New model	683	462	394	226	1765
	Fixed Cycle	1260	695	610	268	2833
Through puts	New model	1223	1384	1211	1279	5097
	Fixed Cycle	1169	1192	1027	1003	4391

(b) oversaturated condition (V/C = 1.0)

V/C=1.0		int 1	int 2	int 3	int 4	total
queue length	New model	1568	943	1193	677	4381
	Fixed Cycle	1681	1127	1327	651	4786
Throughputs	New model	1545	1362	1473	1776	6156

5.2 Comparison with PASSER II and TRANSYT-7F

The performance of the cycle free signal timing produced by the proposed model was compared to PASSER II and TRANSYT-7F. The direct comparison of MOEs produced by the proposed model to those of PASSER II or TRANSYT-7F might be not sufficient for model evaluation because each model has different objective functions and different modeling approaches. Nevertheless, the trend of MOEs may be useful to evaluate the model performance.

Tables 3 and 4 summarized delays and queue lengths produced by the proposed model, PASSER II, and TRANSYT-7F. The MOEs were estimated by respective simulation runs of three models under the same geometric and traffic conditions explained in the experimental design section.
In the delay comparison, the proposed model and TRANSYT-7F produced similar levels of delays on the normal condition (v/c=0.7). On the oversaturated condition, the cycle free signal timings produced superior results (small delays) comparing to those of PASSER II or TRANSYT-7F. It shows that the cycle free signal timing could be a good signal control strategy under saturated conditions.

The average queue length analysis in figure 9 also represents similar results as delay comparison. The proposed model produced better results (smaller queue lengths) than PASSER II, especially under the oversaturated conditions.

<Table 3> comparison of delays (sec/veh)

Comparison Of delay		New model	PASSER-Ⅱ	TRANSYT-7F
V/C = 0.7	int 1	28.0	138.5	28.1
	int 2	28.4	137.74	29.3
	int 3	27.5	31.15	27.7
	int 4	26.3	32.12	28.5
V/C = 1.0	int 1	60.2	124.14	196.2
	int 2	58.1	123.95	194.4
	int 3	56.3	293.76	195.5
	int 4	59.1	293.86	195.1

<Table 4> comparison of queue lengths

		V/C = 0.7								V/C = 1.0							
		int. 1		int. 2		int. 3		int. 4		int .1		Int. 2		int. 3		int. 4	
		N	P	N	P	N	P	N	P	N	P	N	P	N	P	N	P
flow movement	1	1	7	0	7	2	5	0	5	0	87	0	87	11	52	1	52
	2	32	10	15	10	5	7	12	7	50	262	5	262	21	98	4	98
	3	0	3	0	3	0	3	0	3	1	5	0	5	2	5	2	5
	4	5	172	7	172	6	6	9	6	15	187	23	187	17	62	20	62
	5	1	7	1	7	0	5	0	5	15	87	0	87	0	52	0	52
	6	0	10	0	10	0	7	0	7	0	262	2	262	4	98	0	98
	7	0	3	0	3	0	3	0	3	0	5	1	5	1	5	1	5
	8	6	5	9	5	4	6	9	6	23	8	24	8	18	62	24	62

6. CONCLUSIONS

The purpose of this study is to setup a signal optimization procedure using genetic algorithm and to develop a cycle-free based, coordinated dynamic signal timing model for minimizing delay based on Third-generation control concept. The performance of cycle-free signal timings was evaluated in movement-by movement comparisons. The methods for measuring model performance are the number of queued vehicles at the end of green time for each movement, and the number of vehicles passing through the intersection. The result shows that the cycle free signal timing is superior to the fixed signal timing to manage traffic flows of intersections.

This research was an initial attempt to develop a cycle-free based, coordinated dynamic signal timing model. Further research is recommended to enhance the proposed model as follows:

(1) Field validation on a real network is necessary to confirm the benefits of the proposed model.
(2) An optimization algorithm for minimizing queue length is required to manage oversaturated conditions.

The proposed model can produce signal control variables such as cycle length, green time, and offset in a cycle-by-cycle basis. Thus the model can provide more effective control strategies for managing traffic flows on arterial networks. It is expected that the model developed in this research will obtain wide acceptance in conjunction with the signal control systems in the traffic control field.

REFERENCES

U.S. DOT. **Traffic Control Systems Handbook**, Federal Highway Administration. U.S. NTIS.

K.G Courage and C.J. Wallace, **TRANSYT-7F User's Guide**, Transportation Research Center, University of Florida, Gainesville, Florida. December 1991.

J. D. C. Little and M. D. Kelson, **Optimal Signal Timing for Arterial Signal System**, Federal Highway Administration. December 1980.

N. H. Gartner, S. F. Assmann, F. Lasaga, and D. L Hou, A MULTIBAND Approach to Arterial Traffic Signal Optimization, **Transportation Research**, Vol 25B, pp 55-74. 1991.

E. C. P. Chang and C. Messer, **PASSER II-90 Program User's Guide**, Taxas Transportation Institute, Taxas A& M University. June 1991.

R. D. Bretherton, SCOOT Information, Presentation to Traffic Control Delegation in Korea. 1990.

P. R. Rowrie, **SCATS : Sydney Co-ordinated Adaptive Traffic System**, RTA. 1990.

Sumitomo Electric Industries. Traffic Control Systems in Japan. 1990.

Road Traffic Safety Association. Development of a Traffic Adaptive Signal System. 1993.

Federal Highway Administration, Urban Traffic Control / Bus Priority System Third Generation System Software Documentation, Vols. 1-V1, Report Nos. FHWA-RD-76-154/ 159, Washington, D. C. May 1976.

Nathan H. Gartner, Chronis Stamatiadis, and Philip J. tarnoff, Development of Advanced Traffic Signal Control Strategies for Intelligent Transportation Systems : Multilevel Design, **TRR 1494**. 1995.

MacGoWan. J., and I. J. Fullerton, Development and Testing of Advanced Control Strategies in the Urban Traffic Control System. **Public Roads**, Vol.43(NOS. #3). 1979-1980.

TRB, **Highway Capacity Manual**, Special Report 209, 3rd Edition, 1994.

Park B.K., Development of Genetic Algorithm-Based Signal Optimization Program for Oversaturated Intersection, Texas A & M University, 1998.